

KG-GI-PVA Semi-IPN Microspheres: Synthesis, Characterisation, BBY Adsorption And Potential Applications

Arun Kumar*¹, Anjali Goel¹, Vipin kumar²

*¹Department of Chemistry, Gurukul Kangri Vishwavidyalaya, Haridwar, India

¹Department of Chemistry, Kanya Gurukul campus Gurukul Kangri Vishwavidyalaya, Haridwar, India

²Department of Pharmaceutical Sciences, Gurukul Kangri Vishwavidyalaya, Haridwar, India

Email: sharmadibru@gmail.com

Abstract:

Glutaraldehyde crosslinked semi-interpenetrating polymeric network (SIPN) microspheres of katira gum (KG) and polyvinyl alcohol (PVA) has been synthesized by using water in oil emulsion technique. Spherical shape of prepared microspheres was studied by Labovision microscope fitted with micam 2.0 digital camera. Modification in functional groups and structure was studied by FTIR spectroscopy, ¹H NMR and X-ray diffraction. Thermal properties were studied by Thermogravimetric analysis and Differential Scanning Calorimetry. Surface charge and particle size of microspheres were also studied in order to predict their potential applications. Kinetics of swelling for SIPN was investigated in the aqueous solution of different pH. Prepared SIPN were used as micro-particulate devices for adsorptive removal of Bismark Brown-Yellow dye at 5 ppm concentration from water upto 96.92 % by 7 g/L dose. Adsorption followed pseudo second order kinetics and Freundlich isotherm model more closely. Thermodynamic data revealed spontaneity ($\Delta G^\circ = -1.9, 3.5, \& 4.0$ KJ/mol) and endothermic nature ($\Delta H^\circ = 29.22$ KJ/mol) of adsorption at studied temperatures with positive entropy ($\Delta S^\circ = 103.53$ J/mol).

Keywords: SIPN, Katira Gum, Microspheres, Surface Charge, W/O emulsion, Thermal Stability

1. Introduction

Azo dyes are notorious carcinogens due to the presence of aromatic moiety. Even trace amounts of dyes in water can damage its vitality and appearance significantly. The release of colored effluents has triggered a major concern for aquatic lives and human health via the food web and biomagnification. Azo dyes are one of the major sources of water pollution among wastewater discharge, so their removal from various industrial wastewater is of great necessity [Crini, 2006]. There are various methods available for the removal of a wide range of dyes from wastewater. But

adsorption is a promising method due to its efficacy, ease of operation as well as suitability for various types of dyes [Asgher & Bhatti, 2012, Dotto & Pinto, 2011].

Katira gum is plentiful and naturally arising hydrophilic heteropolysaccharide obtained from the bark of the *Cochlospermum religiosum* plant, which is found in India from Uttarakhand to West Bengal. Components and the detailed structure of katira gum was determined by Ojha et al., 2008. Natural polymers can be easily modified to adsorbing membranes, hydrogels, microparticles, semi and full IPN's [L. Li et al., 2014, X. Luo et al., 2015]. Polysaccharides-based materials are of great concern among researchers for adsorption purposes due to their advantageous properties like adsorption efficacy, renewability, eco-friendly nature, biodegradability, and biocompatibility [A. Gandini 2009, Yang et al., 2014, Wang et al., 2004b, Bhatt et al., 2021]. Semi or full interpenetrating polymer networks are an artless and viable route to build polysaccharides-based useful materials in which one polymer penetrates other cross-linked polymers without chemical bonds. SIPN is defined as the arrangement of two polymers (one in a network form and the other in linear form), one of which is synthesized or cross-linked in the immediate presence of the other without any chemical bond between them. SIPN structure helps us to improve many disadvantages of hydrogels like poor mechanical strength, low swelling, solubility. These polymer blends are prepared by mixing two or more polymers [Mamoni et al., 2012]. Natural polymer-based semi interpenetrating polymer networks (SIPN) and interpenetrating polymer networks (IPN) are attracting researchers because of their applicability in various fields like medical science, pharmaceuticals, and environmental reclamation due to their non-toxicity biocompatibility, and versatile functionality [Wang et al., 2004a]. This is because these materials are developed by the entanglements of two different polymer networks and develop some new properties which are not found in any of the individual polymer network [Matricardi et al., 2006]. The interlinked structure of such materials increases their stability, thereby inculcating mechanical strength. These materials are also found to have various functional groups, a porous structure that allows the diffusion of solute particles. This property makes them good adsorbent for dyes and heavy metal ions from aqueous solution.

In the present work katira gum (Natural polymer) and poly vinyl alcohol (Synthetic polymer) based semi-IPN microspheres crosslinked by glutaraldehyde were successfully prepared by water in the oil emulsification method. Further, prepared semi-IPN were characterised by FTIR, TGA, DSC, XRD, ^1H NMR, Labovision microscope, particle size, and zeta potential instrumental techniques. Further, swelling of prepared SIPN microspheres was studied in the aqueous solution at pH 2,7 and 10. Pseudo first and pseudo second order kinetic models were applied to understand the mechanism of swelling. Also, fields in which such materials have been used so far are also discussed to justify the applicability of SIPN prepared in this work.

2. Experimental

2.1. Materials:

Katira gum was purchased from Durga pisaikendra, Kankhal Haridwar. Polyvinyl alcohol, Bismark Brown-Y, castor oil, and glutaraldehyde of analytical grade were purchased from Loba Chemie Pvt Ltd Mumbai India. Acetone, Span 80, and n-Hexane of analytical grade were purchased from Himedia laboratories Pvt Ltd Mumbai India. Distilled water was used in the various process where required.

2.2. Synthesis of KG-gI-PVA semi-IPN microspheres:

Synthesis of semi-IPN microspheres was carried out by water in the oil emulsion technique without using any costly and hazardous chemicals. Katira gum was powdered and passed through sieve number 120 to prepare its gel in distilled water and polyvinyl alcohol was dissolved separately in hot distilled water at 75 °C. Now, gel of katira gum and PVA solution were mixed in different ratio and transferred to a beaker having approximately 300 ml castor oil at 70 °C. Oil phase had one % span 80, in it to emulsify the aqueous and oil phase. Further, contents of beaker mechanically stirred for ten minutes at 80 °C then crosslinking agent glutaraldehyde was added drop-wise in the beaker. This mixture was stirred for six hours at around 80 °C and 2000 rpm. After the stirring of six hours hardened semi-IPN microspheres were formed and settled down in the beaker. Microspheres were separated from castor oil simply by decantation process. The remaining castor oil and unreacted glutaraldehyde were removed by washing several times with n-hexane and acetone respectively. Finally, microspheres were washed with glycine to remove traces of unreacted glutaraldehyde, if any. Thus, obtained Semi-IPN microspheres were dried in a hot air oven for 24 hours at 45 °C and stored in an airtight container for further use.

2.3 Characterization:

2.3.1 FTIR Analysis:

Dried microspheres and katira gum were tableted with KBr in a weight ratio of 1/ 100 to record FTIR spectra (FTIR Model IR-Perkin Elmer, Spectrum 2000) in the range of 400–4000 cm^{-1} .

2.3.2 Thermal Analysis:

TGA of KG and SIPN were done to investigate the thermal properties and weight losses at different degradation stages using instrument DTG-60, serial no C30565100650TK. Thermograms were obtained at a heating rate of 5 °C/min in a nitrogen atmosphere with a flow rate of 100 ml/min in the temperature range from 24 to 600 °C. DSC analysis was also carried out for both KG and SIPN on the Instrument-Perkin Elmer-USA model JADE DSC. The temp was varied from - 40 to 300 degrees

centigrade at the rate of 10-degree cent per minute during the study. The purged gas during the study was nitrogen at the flow rate of 20ml/min.

2.3.4 X-ray diffraction:

KG and microspheres were pre-dried in a vacuum oven at 45 °C for 24 h to remove remaining moisture. The crystallinity index of the samples was measured using an X-ray diffractometer (XRD; XD-2, Beijing Purkinje General Instrument Co., Ltd., Beijing, China) with Cu target at 36 kV and 20 mA. Samples were tested in the angular range of $2\theta = 5\text{--}80^\circ$ with a scanning rate of $2^\circ/\text{min}$.

2.3.5 Nuclear Magnetic Resonance (^1H NMR)

For KG and microspheres ^1H NMR were recorded on 500 MHz Bruker Advance II-500 equipped with One NMR probe. ^1H NMR chemical shifts (δ) were reported in parts per million (ppm) and data was handled with Mestrelab Research software (MNova 14.2.1).

2.3.6 Particle size analysis:

The KG and SIPN were dispersed in ethylene glycol and taken in a glass cuvette for the determination of particle size at 25 °C using a Malvern, Zetasizer Version 7.11 Serial Number: MAL1112196, instrument at count rate 9.7 kcps, measurement position 4.65 mm, for 50 seconds.

2.3.7 Zeta potential determination:

Zeta potential KG and semi-IPN microspheres measured by dispersing it in water and taken in the clear disposable zeta cell at 25 °C using a Malvern, Zetasizer Version 7.11 Serial Number: MAL1112196 instrument at count rate 267.1 kcps, measurement position 2.00 mm, for 10 zeta runs. The measurements were done in triplicate for each sample and the average values are reported.

2.3.8 Morphological study:

Spherical shape and closer look at the surface of SIPN was observed with the help of Labovision microscope, (T/F E Glass Germany) fitted with micamUSB 2.0 at 10x and 40x resolutions. Few particles of samples were taken on the slide having a drop of castor oil to obtain clear microscopic images

2.4 The swelling behavior of SIPN:

The swelling of native KG and microspheres was determined gravimetrically at 25 °C. Dry and accurately weighed samples were put into different test tubes having an equal volume of distilled water at definite pH to reach equilibrium swelling. At regular time intervals, samples were taken out

from aqueous media, and excess water was carefully removed with tissue paper without squeezing the sample. Then, the masses of swollen samples were carefully determined by electronic balance. The swelling ratio (SR) was calculated by using following formula [H. Tu et al., 2017].

$$SR(\%) = \frac{(W_s - W_d)}{W_d} \times 100$$

Where W_s and W_d are the weight of swollen and dry samples respectively.

Water absorption data were analyzed with pseudo first-order and second-order kinetics by following equations [Yilmaz & Pekcan, 1998, Katime et al., 2001].

$$\ln \left[\frac{W_f}{W_f - W_t} \right] = K_1 t$$
$$\frac{t}{W} = \left[\frac{1}{(K_2 W^2 f)} \right] + \frac{t}{W_f}$$

Here W_f is the maximum water taken by samples W_t is the water taken at time t , and K_1 and K_2 are specific rate constants.

Batch adsorption experiments:

Batch mode adsorption experiments were performed to study the removal Bismark Brown-Yellow (BBY) double azo dye from aqueous solution by semi-IPN microspheres. Experiments were carried in 30 mL stoppered tube by taking 40 mg adsorbent in 20 mL dye solution and agitated at 120 rpm in the water bath shaker. The influence of adsorption governing factors such as temperature, dosage of adsorbent, dye concentration, contact time, and pH on the efficacy of dye removal was also studied. Remaining amount of dye in the solution at different time intervals was studied by Shimadzu 1800 UV-VIS spectrophotometer at λ_{max} 460.5 nm. The percent dye removal and dye removed at equilibrium by prepared SIPN was calculated using the equation given herein (S. Zhao et. al., 2012).

$$q_e = \frac{(C_i - C_e)V}{m}$$

$$R \% = \frac{(C_i - C_e)100}{C_i}$$

Here C_i is concentration of dye initially present in the solution (mg/L), C_e is residual concentration of dye at equilibrium (mg/L), Volume of dye solution is V (L), and mass of adsorbent used is m (g)

3. Result and Discussion:

3.1 Synthesis of SIPN:

Semi interpenetrating polymer network microspheres were synthesized by crosslinking katira gum and polyvinyl alcohol by glutaraldehyde. Crosslinking took place via a condensation reaction between the –OH functional group of katira gum and polyvinyl alcohol with –CHO functional group of glutaraldehyde via acid-catalyzed nucleophilic addition reaction **figure 1**. In the first step protonation of –CHO oxygen takes place, which makes it a better electrophile. Now, in the rate-determining step lone pair of –OH from PVA and KG can attack on the carbon atom of protonated –CHO group via nucleophilic addition to give hemiacetal, followed by elimination of water molecule due to the attack another adjacent –OH. This reaction leads to the formation of six-membered acetal with PVA and five-membered acetal with D- galactose of the KG polymer network during crosslinking reaction. However, no catalyst was added from outside since –COOH moieties in katira gum, dissociates to furnish the catalytic amount of H⁺ ion in the reaction medium to derive the reaction.



D – Galacturonic acid moiety of KG

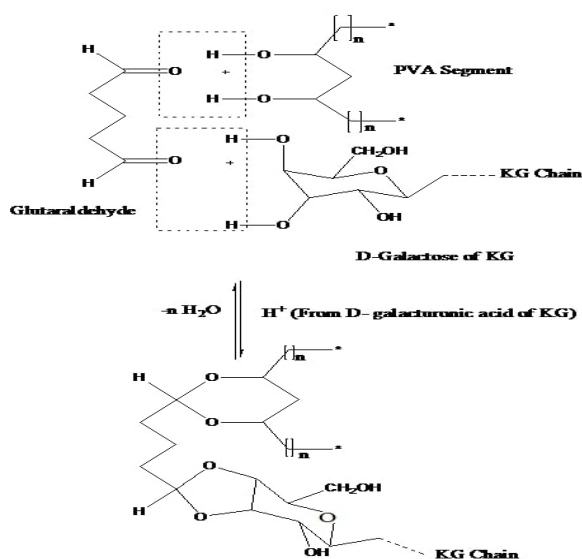


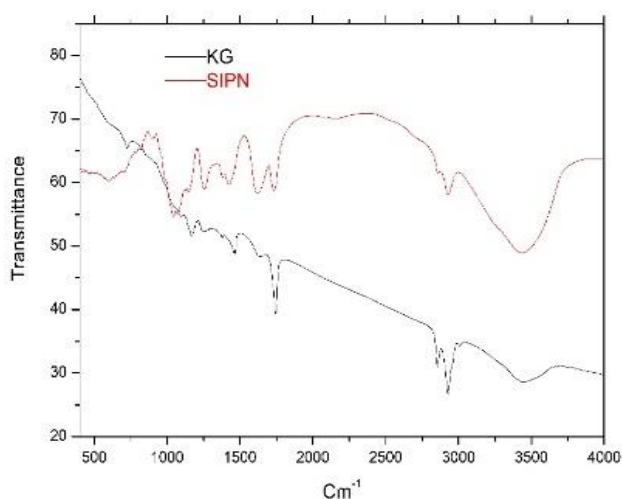
Fig. 1: Crosslinking reaction of KG and PVA with glutaraldehyde.

3.2 FTIR Analysis:

The FTIR spectra of katira gum and semi-IPN microspheres are given in the **figure 2** which shows the broad peak at 3437 cm⁻¹ due to –OH stretching vibrations. Broadening of peak of semi-IPN in the range from 3500 to 3200 cm⁻¹ is also due to inter and intra molecular hydrogen bonding of –OH

group of PVA [Herman et al., 2008]. Two bands in the range of 2830 to 2700 cm^{-1} is due to C-H of glutaraldehyde. PVA-glutaraldehyde, C-O-C linkage appears to be in the FTIR spectra at 1150-1085 cm^{-1} [Herman et al., 2008] which confirm the crosslinking to form SIPN microspheres. The peak that appeared in the range of 1630 and 1042 cm^{-1} is attributed to $-\text{CH}$ and $-\text{CH}_2$ in-plane bending vibrations. The band at 1726 cm^{-1} is due to stretching vibrations of $>\text{C}=\text{O}$ groups in $-\text{COOH}$. Transmittance observed at 1110 cm^{-1} corresponds to $-\text{C}-\text{O}-\text{C}-$ stretching from acetal linkage and glucopyranose ring. Also, the broadening of $-\text{OH}$ stretching peak in the FTIR spectra of semi-IPN indicates the crosslinking of katira gum and PVA by glutaraldehyde.

Fig. 2: FTIR Spectra of SIPN and katira gum.



3.3 Thermal analysis:

The TGA and DSC thermograms of raw exudate and SIPN are given in **figure 3 and 4** respectively. Crosslinking can also be supported by TGA and DSC thermogram since thermal stability of SIPN should increase after crosslinking [Xinyu et al., 2014]. During the thermal analysis raw katira gum shows onset of first degradation stage from 34.87 $^{\circ}\text{C}$ till 79.22 $^{\circ}\text{C}$ with 17.55 % weight loss whereas semi-IPN shows onset of first degradation stage from 80.25 $^{\circ}\text{C}$ till 155.14 $^{\circ}\text{C}$ with only 6.37 % weight loss that means semi-IPN has formed with more thermal stability. Second decomposition stage for katira gum starts from 238.49 $^{\circ}\text{C}$ till 278.19 $^{\circ}\text{C}$ with 43.47 % weight loss but for semi-IPN it is from 255.70 $^{\circ}\text{C}$ till 279.93 $^{\circ}\text{C}$ with 37.26 % weight loss. This fact is also supported by DSC thermograms of semi-IPN and katira gum. After crosslinking in SIPN the peak is found at 116.61 $^{\circ}\text{C}$ with peak height 5.3356 mW and for katira gum peak is at 109.53 $^{\circ}\text{C}$ with peak height 29.866 mW. This can be attributed to crosslinking and formation of more thermally stable semi-IPN microspheres.

Fig. 3: TGA Thermogram of SIPN and katira gum

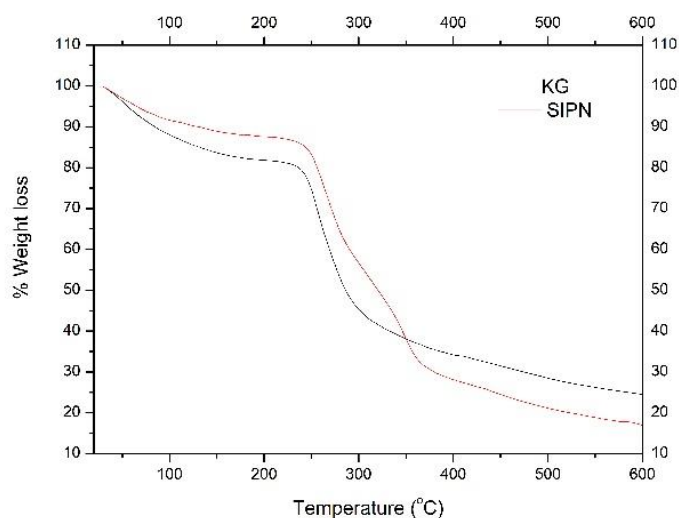
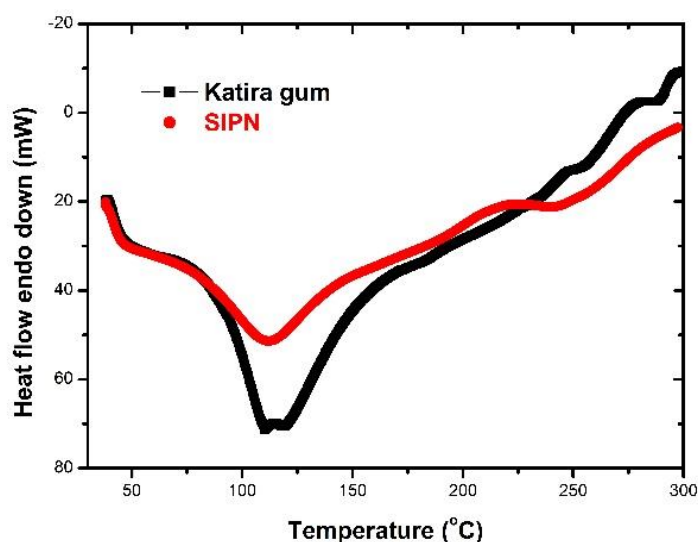


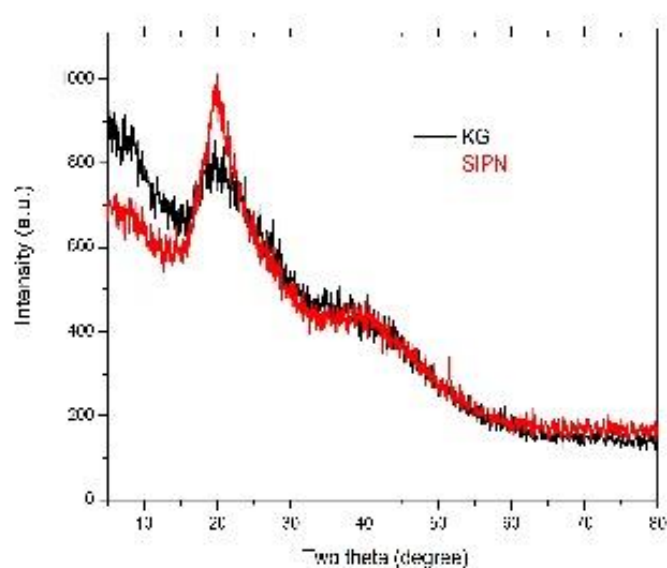
Fig. 4: DSC Thermogram of SIPN and katira gum



3.4 XRD analysis:

The XRD patterns of native katira gum and KG-gl-PVA semi-IPN microspheres are shown in the **figure 5**. The broad diffraction peak in the XRD plot of katira gum is found to be at $2\theta = 21.68^\circ$, and for semi-IPN, comparatively narrower diffraction pattern is obtained at $2\theta = 19.69^\circ$ indicating the crosslinking of katira gum backbone [Jana et al., 2018].

Fig. 5: XRD pattern of SIPN and katira gum



3.5 Nuclear Magnetic Resonance (^1H NMR)

^1H NMR of katira gum and prepared microspheres is shown in **figure 6 and 7** respectively. It was done in order to investigate the change after crosslinking which is evident from the mere observation of both the spectra. Spectra of katira gum shows mainly the doublet at δ 4.89 ppm with intensity ratio 1:1, singlets at δ 4.6 ppm due to hydrogen at first carbon of D-galacturonic acid and L-rhamnose (Ojha et. al., 2008) and a triplet at δ 2.2 ppm with Pascal triangle intensity ratio 1:2:1. Whereas, spectra of SIPN shows several other spikes also out of which peak at δ 4.68 ppm is due to proton of hemiacetal or acetal structure, (Hansen et. al., 1997) indicating the crosslinking between KG and PVA by glutaraldehyde. The triplet around δ 2.3 ppm in both the spectrums are due to methylene hydrogens (Hansen et. al., 1997). The peaks around δ 4.2, 3.8 ppm are due to proton of CH-OCO in crosslinking.

Fig. 6: ^1H NMR spectra of KG

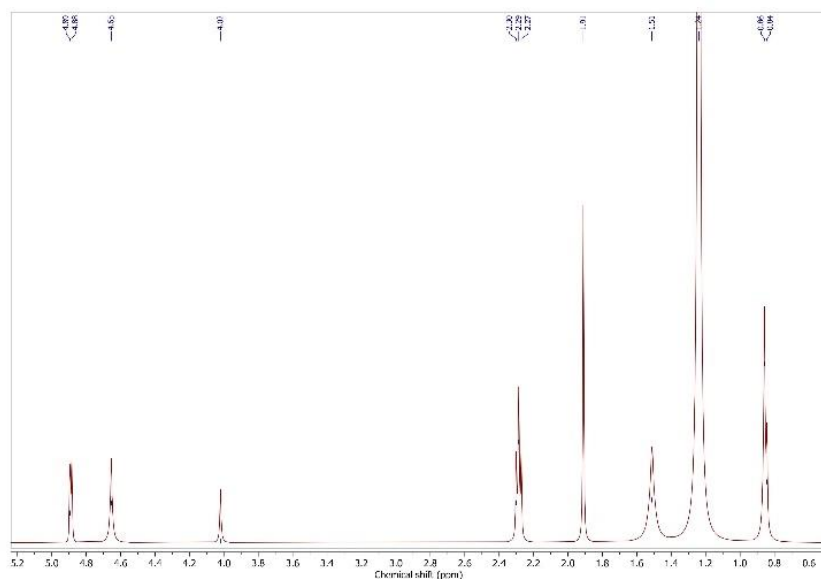
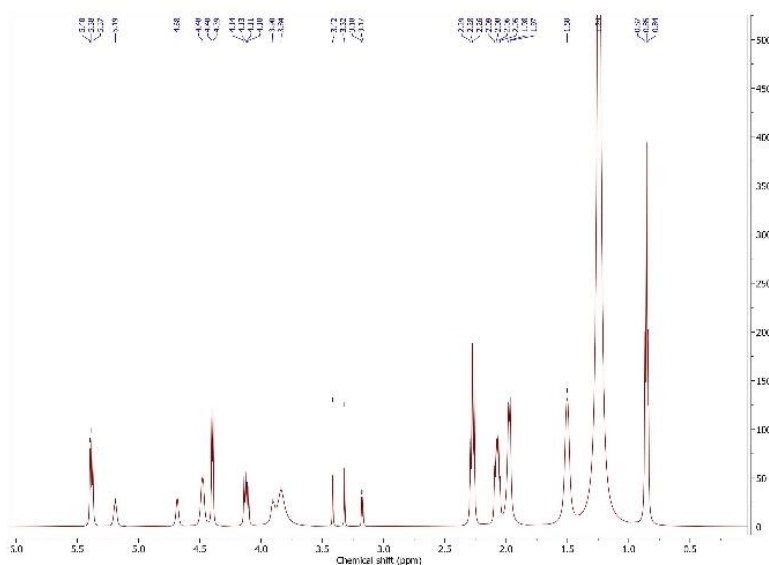


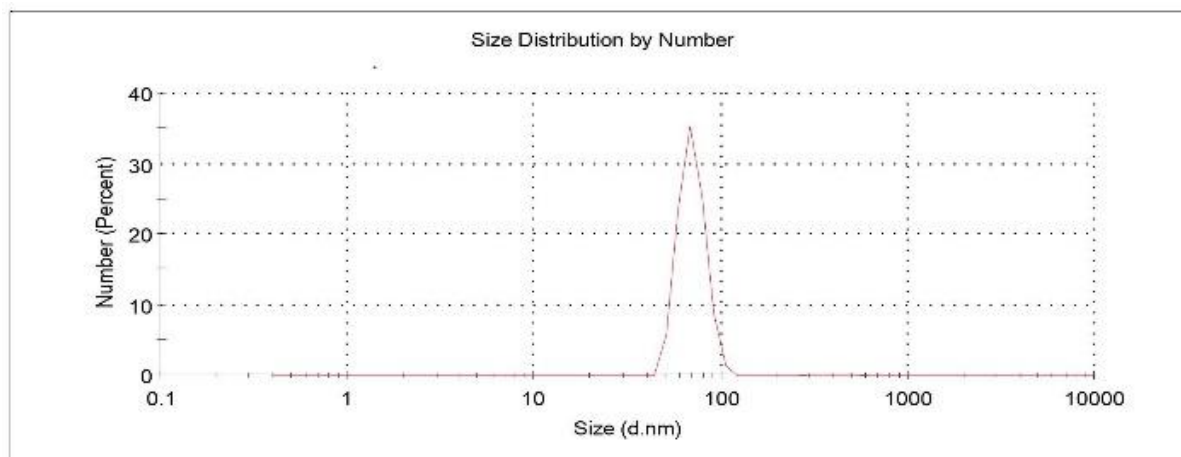
Fig. 7: ¹H NMR spectra of SIPN



3.6 Particle size analysis:

The particle size distribution of prepared SIPN microspheres was analysed at 25 °C by dynamic light scattering which is given in the **figure 8** and Z-average was found to be 259.3 (d. nm) with polydispersity index 0.374 indicating the uniform size distribution of microspheres in this z-average range. Peak one shows 0.4 % particles having size distribution by number 429.4 (d. nm) with standard deviation 106.5 whereas second peak shows 99.6 % particles having size distribution by number 70.15 with standard deviation 11.35 (d. nm).

Fig. 8 Particle size distribution plot of SIPN



3.7 Zeta potential determination:

Zeta potential of prepared microspheres was also determined at 25 °C is given in the **figure 9** and it was found to be -6.95 mV with conductivity 0.181 m S/cm. The only peak was observed in the zeta potential distribution plot at above mentioned value having 100 % area with standard deviation 5.13 mV. Zeta potential distribution plot of katira gum shown in figure 10 have two peaks and the zeta potential was found to be -6.06 mV. Surface charges on kg and SIPN were found to be negative with similar magnitude. The negative charge on the surface of microspheres may be attributed to the ionisation of carboxylic group in the dispersant used in the study (Soraya Hassanpour & Massoumeh Bagheri, 2017).

Fig. 9: Zeta potential plot of SIPN

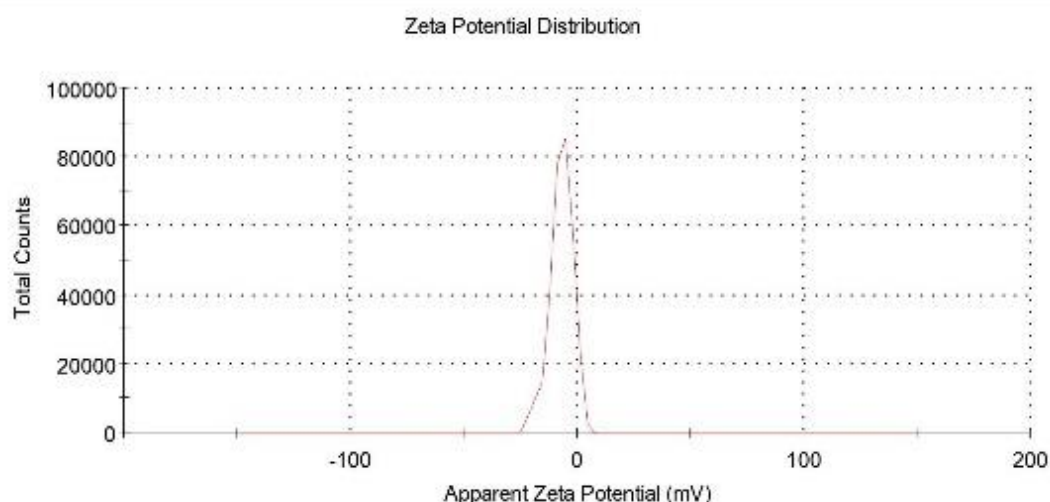
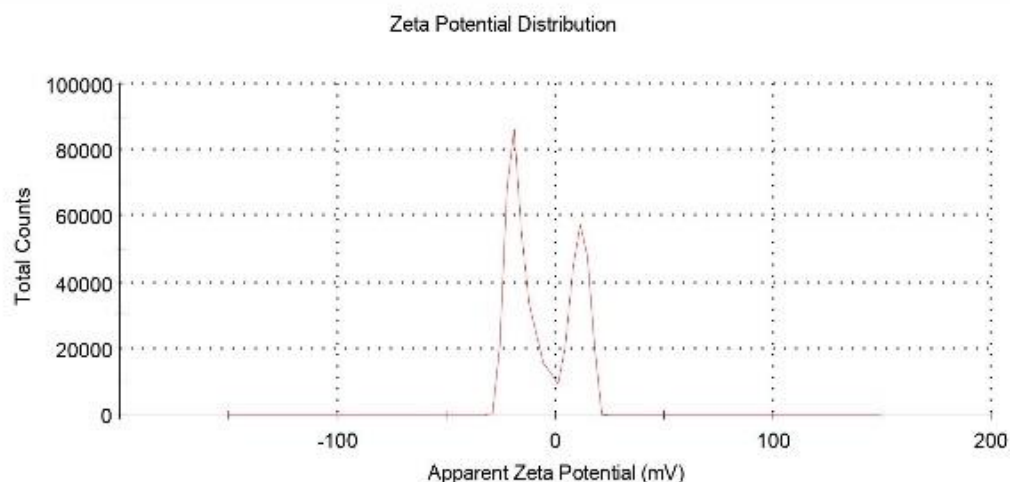


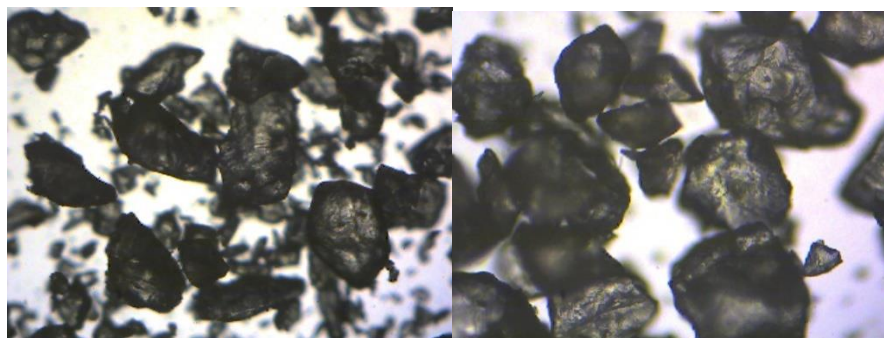
Fig. 10: Zeta potential plot of native KG

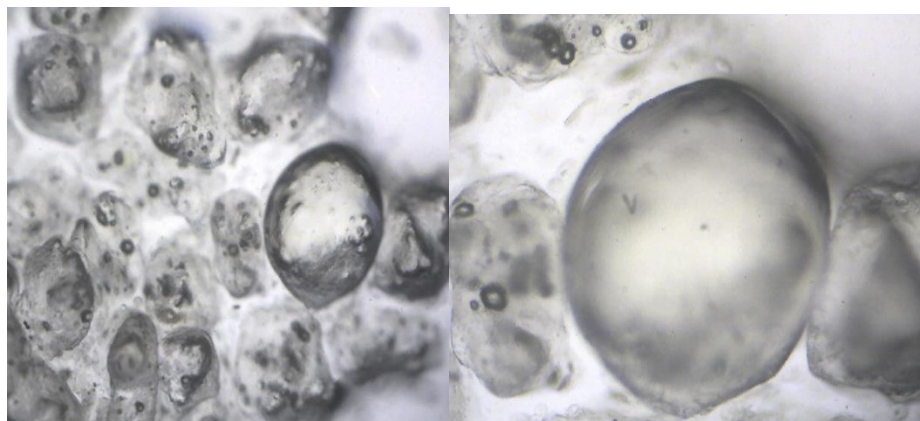


3.8 Morphological study:

Clear difference in the surface morphology of KG and microspheres can be observed in the microscopic images, shown in the **figure 11**. Prepared semi-IPN have spherical shape and rough surface as compared to native katira gum surface. Micrographs of KG powder are shown at 4x and 10x whereas SIPN are shown at 10x, and 100x magnification to have closer look at the surface of microspheres.

Fig. 11: Micrographs of KG and SIPN





3.8 Swelling study:

Swelling experiments were carried out at room temperature (25 °C). Semi-IPN microspheres prepared in the present study show deviation in swelling on changing the pH of the solution due to the ionization behavior of -COOH groups of katira gum in response to solution pH. The influence on swelling behavior for KG and microspheres was investigated at three different pH viz. 2, 7, and 10 depicted in **figure 12**. The pH of the aqueous media was adjusted by 0.1 M HCl and 0.1 M NaOH solutions. Change in swelling with Change in pH of solution is due to the presence of -COOH functionalities in the katira gum and semi-IPN microspheres, which behave differently at different H^+ concentrations. The experimental outcomes can be explained as follow, at pH 2, -COOH group remains unionized and swelling is mainly governed by hydrophilicity and hydrogen bonding of water and semi-IPN microspheres. The maximum water uptake by microspheres at this pH was found to be 598 mg per 100 mg SIPN. On the other hand, at pH 10 most carboxylic acid group ionizes to give negatively charged -COO^- ions in semi-IPN. Electrostatic repulsion between negatively charged -COO^- ions increases the intermolecular spacing, which leads to more water uptake capacity [A. Pourjavadi et. al., 2008, Thakur and Arotiba, 2018]. However, swelling capacity decreases on further increment in the pH due to an increase in the number of Na^+ ions which make pair with -COO^- ions. The maximum water uptake at this pH was found to be 676 mg water per 100 mg of semi-IPN. Finally, swelling at pH 7 was found to be 622 mg per 100 mg semi-IPN which is lower than at pH 10 but higher than at pH 2. It is because at this pH ionization of -COOH is less than pH 10 but more than pH 2. The ionization of the -COOH group starts after pH 5 since the average dissociation constant for carboxylic acids is around 10^{-5} ($K_a = 10^{-5}$ thus $\text{p}K_a = 5$). According to a general rule if $\text{pH} = \text{p}K_a$ then $[\text{RCOOH}] = [\text{COO}^-]$ that means the concentration of ionized and unionized forms are equal. So, without going into calculations we can say that pH 7 is more basic than pH 5 so at pH 7 the concentration of H^+ ions is 100 times lower (two log unit). Hence according to LeChaterlier's principle ionization equilibrium will shift on the right-hand side that means ionization favors. The pseudo first-order and second-order kinetics were applied to identify the swelling kinetics of katira gum and

microspheres. Obtained data and linear fit kinetic plots has been given in **table 1** and **figure 13, 14** respectively. From the value of the correlation coefficient, it can be stated that the swelling of semi-IPN follows second order kinetics at all three pH values.

Table 1: Kinetic data of swelling for KG and microspheres.

	Katira gum swelling kinetics						SIPN swelling kinetics					
	Pseudo first order			Pseudo second order			Pseudo First			Second Pseudo Second		
	K _{1p}	Intercept	R ²	K _{2p}	Intercept	R ²	K _{1p}	Intercept	R ²	K _{2p}	Intercept	R ²
pH2	0.0123	0.437	0.9757	6.20164E-05	0.0853	0.9944	0.0128	0.5268	0.966	9.39457E-05	0.0958	0.995
pH7	0.0128	0.3997	0.976	3.8247E-05	0.0753	0.9905	0.0152	0.6053	0.9629	0.000101294	0.0773	0.993
pH10	0.0132	0.4736	0.9636	5.20064E-05	0.0623	0.9938	0.0147	0.5957	0.8965	0.000106161	0.0633	0.995

Fig. 12: Swelling pattern of KG and SIPN

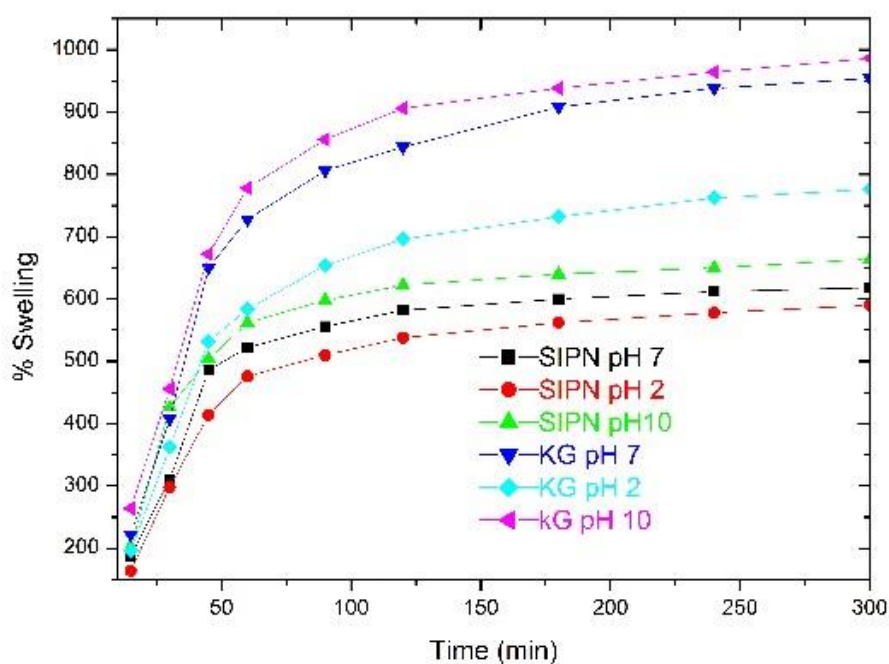


Fig. 13: Pseudo first order kinetic model

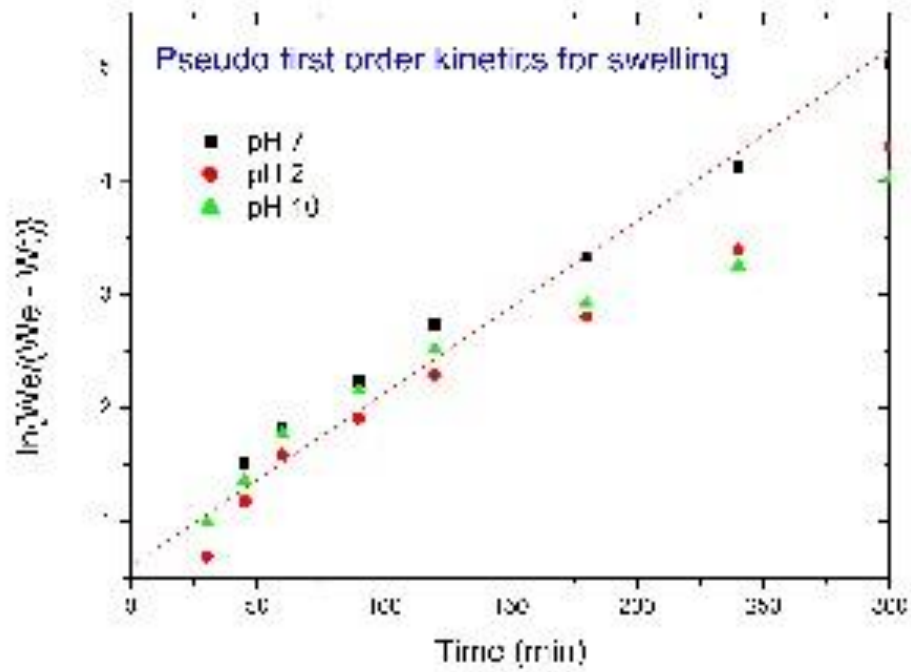
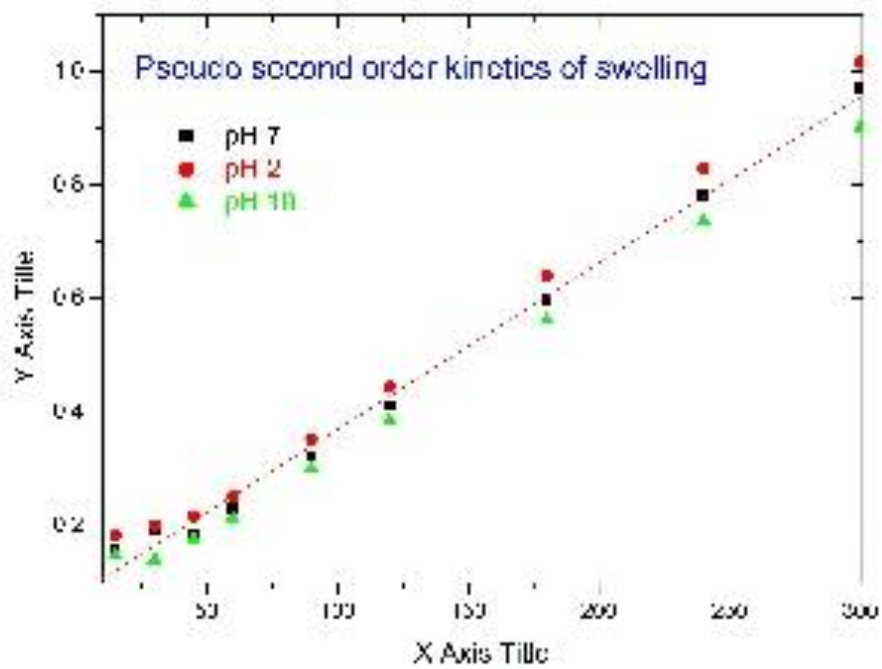


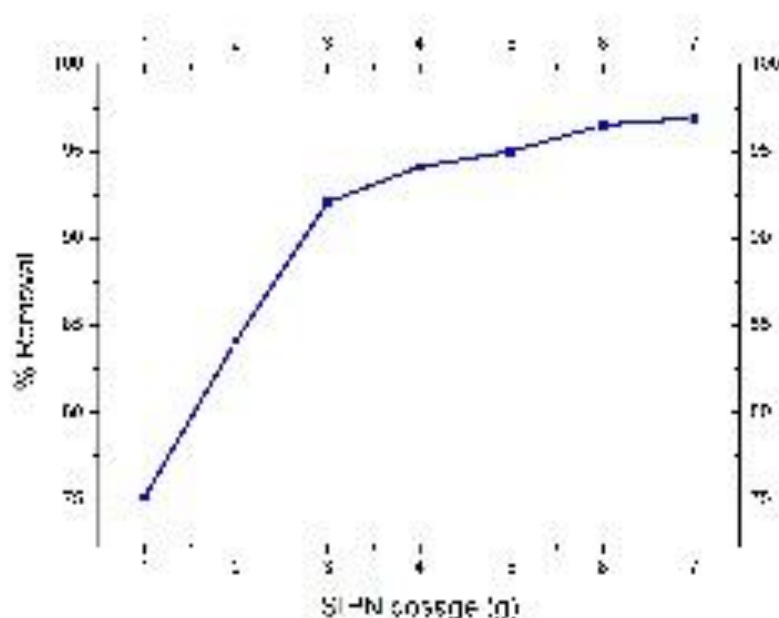
Fig. 14: Pseudo second order kinetic model



4.0 Effect of various parameters on adsorption:

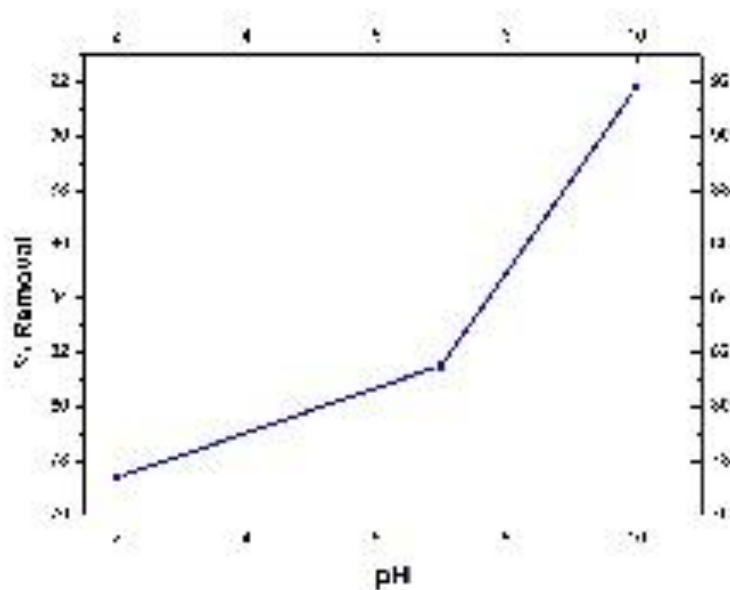
4.1 Effect of adsorbent dose on dye removal The effect of SIPN amount on percent BBY dye removal was analysed by adding altered doses of microspheres as depicted in the **figure 15**. The outcome of the experiments revealed that percent dye removal increases with higher doses of adsorbent. Highest dye removal achieved by 7 g/L dose, was 96.92 % further increase in microsphere dose have no significant improvement in % dye removal. Due to increase in the amount of adsorbent there is an increase in surface area and adsorbing sites which results in more adsorption (M. Ghaedi et. al., 2013).

Fig. 15: Effect of adsorbent dose on % dye removal



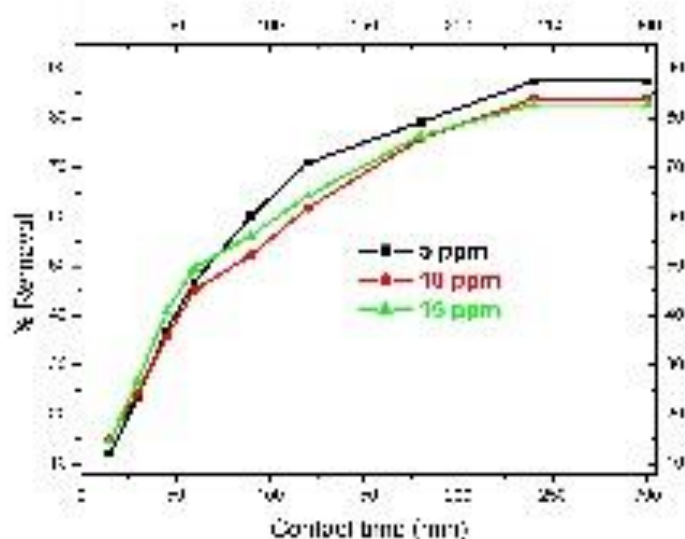
4.2 Effect of pH on adsorption was investigated (**Fig. 16**) by conducting experiments at acidic (pH 2), neutral (pH 7), and basic (pH 10) pH of the solution considering that these values do not cause degradation or loss in the intensity of colour of BBY dye. H^+ and OH^- concentration plays an important role in aqueous chemistry or adsorption since it can lead to protonation or deprotonation of functional groups on the adsorbent surface, which affect the ionic interaction between adsorbate and adsorbent. The most efficient dye removal was observed at pH 10, since SIPN surface negatively charged at this pH due to the ionisation of $-COOH$ group. Zeta potential results has also shown that SIPN surface is negatively charged even at neutral pH. Thus microspheres will attract cationic azo dye BBY more strongly via electrostatic interaction to give more adsorption. Similar reason can be given to explain adsorption at 7 pH. Comparatively less adsorption at pH 2 is due to unionised $-COOH$ groups which results in lesser dye-SIPN attraction.

Fig. 16: Effect of pH on % dye removal



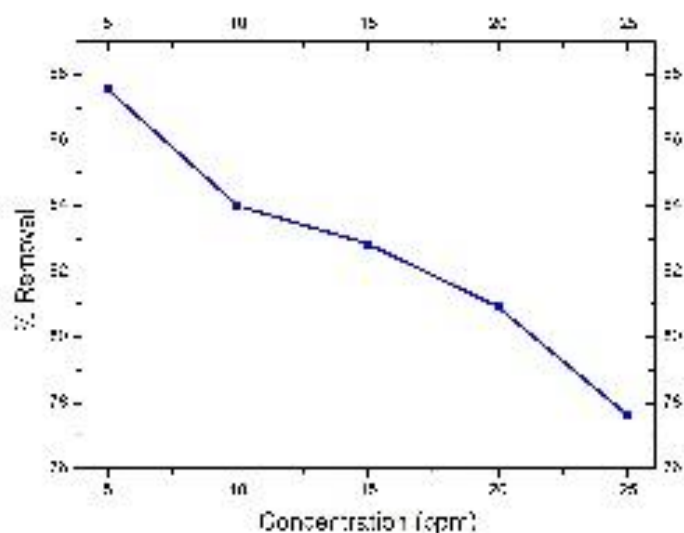
4.3 Effect of contact time on adsorption help us to predict the complete equilibrium state of the process. It was observed that initially dye removal take place rapidly later it goes relatively slower and finally equilibrium was reached around 240 minutes (**Fig. 17**). Fast adsorption in the starting is due to availability of more adsorption sites, speedy swelling of SIPN, and opposite charges on adsorbent and adsorbate. With the consumption of adsorbent sites adsorption process gets slower and finally attains equilibrium.

Fig. 17: Effect of contact time on % adsorption



4.4 Initial dye concentration also found to affect percent dye removal (**Fig. 18**). This effect was studied by taking different initial dye concentration. As initial dye concentration is increased adsorption capacity also increased but after certain point reaches a plateau. This is due to large number of dye molecules are available to bind with sites of adsorbent. It increases the amount of dye adsorbed but percent dye removal will decrease, which is due to repulsion between dye molecules and engagement of available adsorbing sites at higher concentrations of dye (S. Zhao et. al., 2012). It can be concluded from the results that SIPN shows higher dye removal at lower (5 mg/L dye) concentration.

Fig. 18: Effect of initial dye concentration



4.5 Kinetics of adsorption:

The type of mechanism by which adsorption took place can be explained with the help of best fit kinetic model. In determination of efficiency of adsorption process, knowledge of its kinetics is important. Two kinetic models, viz pseudo first and second order, were applied on adsorption data. The linear form of these kinetic models are given below.

$$\log(q_e - q_t) = \log q_e - \frac{K_1 t}{2.303}$$

Here q_t is amount of dye adsorbed (mg/g) at time t and q_e is the dye adsorbed at equilibrium. Time is shown by t and K_1 represents the rate constant for pseudo first order kinetics (1/min). The linear plot of $\log(q_e - q_t)$ vs. t give the value of slope, intercept and K_1 . In this kinetic model q_e does not denote the actual number of adsorption sites and intercept of the plot is not always equal to $\log q_e$.

The linear form of pseudo first order kinetic model, which mainly represents the chemical adsorption is given as below

$$\frac{t}{qt} = \frac{1}{qe2K2} + \frac{t}{qe}$$

Here q_e , q_t have their usual meaning as mentioned above, and K_2 (g/mg min) represents the rate constant for pseudo second order kinetics. The linear plot of t/q_t vs. t gives the value of slope, intercept, and K_2 . The data obtained from kinetic models and values of q_e mg/g calculated are given in the **table 2 and 3** respectively. The value regression constant (R^2) predicts the best fit model for the process. It is clear from the table that the value of R^2 is more for pseudo second order kinetics it suggest that dye removal process may be chemical adsorption type. Also the value of experimental and calculated adsorption capacities (q_e) are closer in case of pseudo second order kinetic model.

Table 2: Pseudo first and second order kinetic data of adsorption of BBY by SIPN.

Pseudo 1	5 ppm			
Intercept	slop	qe(cal.) (mg/g)	K₁	R²
1.2001	-0.0196	3.320449	-6.53333E-05	0.9416
Pseudo 1	10 ppm			
Intercept	slop	qe(cal.) (mg/g)	K₁	R²
1.4823	-0.0112	4.403061	-3.73333E-05	0.9738
Pseudo 1	15 ppm			
Intercept	slop	qe(cal.) (mg/g)	K₁	R²
1.8335	-0.0127	6.255743	-4.23333E-05	0.9736

Pseudo 2	5 ppm				
Intercept	slop	qe(cal.)	qe2	K₂	R²

		(mg/g)			
36.324	0.3134	3.19081	10.18126994	0.002704	0.9709
Pseudo 2	10 ppm				
Intercept	slop	qe(cal.) (mg/g)	qe2	K₂	R²
17.702	0.1724	5.800464	33.64538283	0.001679	0.9932
Pseudo 2	15 ppm				
Intercept	slop	qe(cal.) (mg/g)	qe2	K₂	R²
10.267	0.1219	8.203445	67.29651354	0.001447	0.991

Table 3: Values of experimental extent of adsorption (qe)

Experiment	Ci (ppm)	Ce (mg/L)	qe(exp)(mg/g)
1	5	0.6223	2.18885
2	10	1.6	4.2
3	15	2.57219	6.213905

Fig. 19: Pseudo first order kinetic model

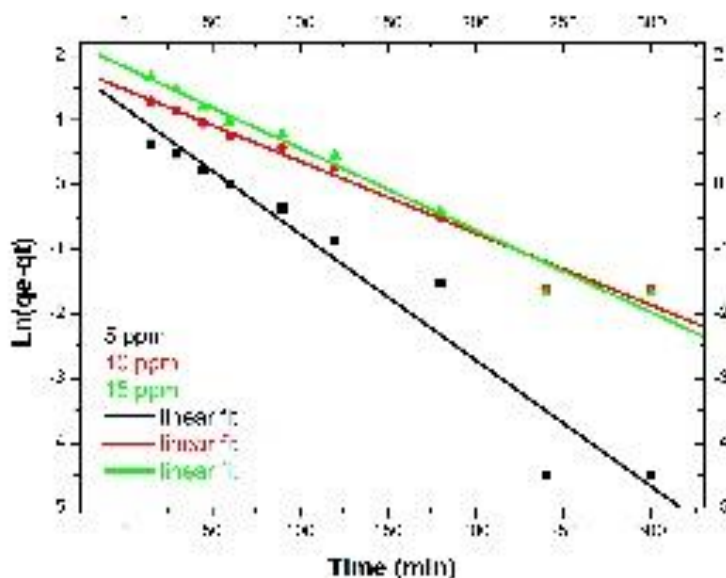
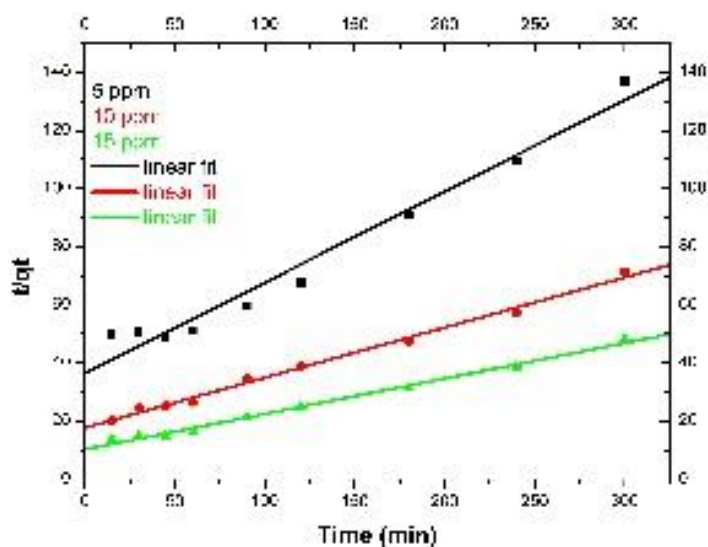


Fig. 20: Pseudo second order kinetic model



4.6 Isotherm modelling for adsorption:

Langmuir and Freundlich isotherm models were applied on adsorption data to assess the type of adsorption. Freundlich isotherm is the vital and initial model of all. It states that adsorption is reversible and are not limited to monolayer. According to this model adsorption is multilayer over heterogeneous surface with non-uniform distribution of adsorption enthalpies. The equation for this model can be expressed as follow.

$$\ln q_e = \frac{1}{nF} \ln C_e + \ln kF$$

Here $k_f(mg^{1-1/n} L^{1/n} /g)$ is Freundlich constant. Adsorption is favourable if value of n_f is between one to ten.

Equilibrium isotherms are the plots which describe the adsorption at constant temperature and pH. Langmuir isotherm model describes monolayer adsorption on the fixed number of adsorption sites in the given mass of adsorbent. If a molecule occupies an adsorption site no other molecule can adsorb at that site. According to Langmuir theory attraction forces decreases rapidly as distance increases between dye and adsorbent. The linear form of Langmuir model can be represented as follow.

$$\frac{C_e}{q_e} = \frac{1}{K_L q_m} + \frac{C_e}{q_m}$$

$$R_L = \frac{1}{(1 + K_L C_0)}$$

Here K_L (L/mg) is Langmuir constant, q_m is maximum monolayer adsorption capacity of adsorbent (mg/g) and C_0 is the highest initial dye concentration. R_L is the important separation factor and is a dimensionless constant. It indicates the favourability of adsorption process.

Adsorption data was tested with Langmuir and Freundlich isotherm models and values are listed in **table 4**. The value of R_L is found to be 0.193, which indicate that the adsorption is favourable according to Langmuir adsorption model (Vaneet et. al., 2018). Which is further supported by value of R^2 (0.989). But Freundlich model is more suitable for the BBY removal.

Table 4: Data for Langmuir and Freundlich isotherm models.

Langmuir	Intercept	Slop	$q_{max}(mg/g)$	K_L	R_L	R^2
	0.0659	0.2374	15.1745068	0.277591	0.193654	0.9895
Freundlich	Intercept	Slop	$1/n$	K_f	R^2	
	0.4938	0.7212	0.7212	3.117	0.9983	

Fig. 21: Langmuir isotherm model

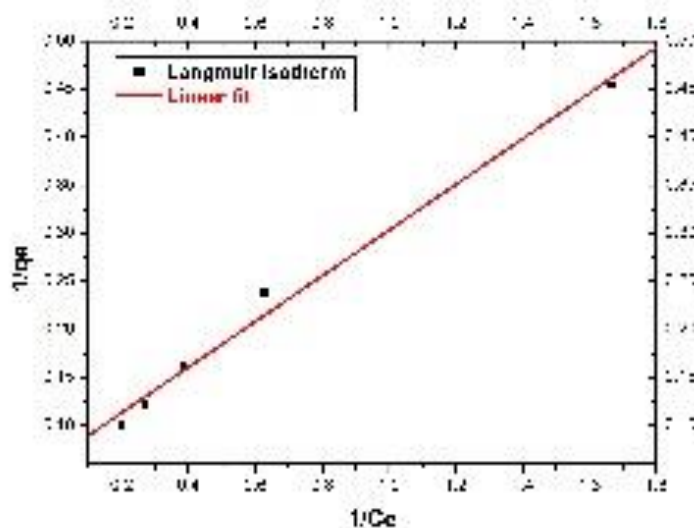
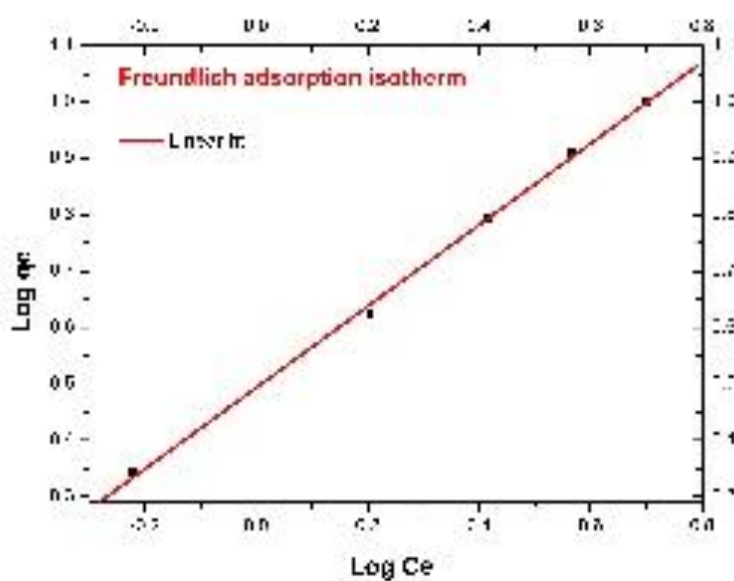


Fig. 22: Freundlich isotherm model



4.7 Study of thermodynamic parameters:

The effect of temperature on any physical or chemical process can be studied with the help of thermodynamic parameters. Adsorption experiment were conducted at 30 °C, 40°C, and 50 °C to find the nature of adsorption process with the help of thermodynamic functions, and their values are given in the **table 5**. The formulas used to find these properties are given below:

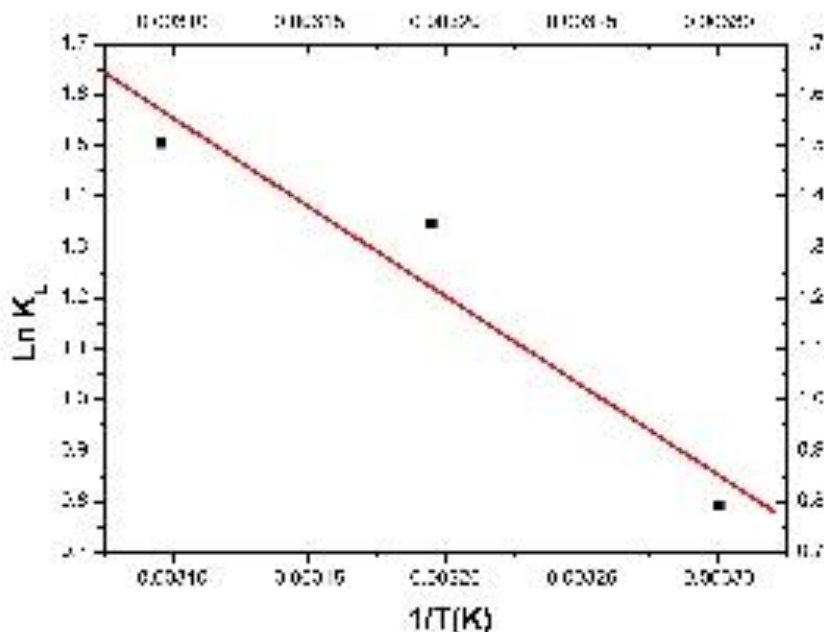
$$\Delta G^\circ = \Delta H^\circ - T\Delta S^\circ$$

$$\Delta G^\circ = -RT \ln K_d$$

$$\ln K_d = -\frac{\Delta H^\circ}{RT} + \frac{\Delta G^\circ}{R}$$

Here K_d is adsorption constant, T is temperature in kelvin scale, ΔG° , ΔH° , and ΔS° have their usual meanings. From **table 5** it can be concluded that adsorption of BBY by semi-IPN is spontaneous at studied temperatures due to negative value of ΔG° . Positive values of ΔH° and ΔS° indicate endothermic nature of adsorption and increased randomness at the boundary of SIPN-solution during adsorption respectively (Ahmed et. al., 2019). Hence adsorption is favoured as temperature increases which is indicated by change in enthalpy value of q_e (mg/g).

Table 5: Values of thermodynamic functions from the linear plot of $\ln K$ against $1/T$



Intercept	Slop	R ²	R(J/mol K)	ΔH° (J/mol)	ΔH° (KJ/mol)	ΔS° (J/mol)
12.453	-3515.6	0.9154	8.314	29228.7	29.2287	103.53424

Temp	T(K)	1/T	Ce	qe	K _L	ln K _L	R ²	ΔG° (j/mol)	ΔG° (KJ/mol)
------	------	-----	----	----	----------------	-------------------	----------------	--------------------------	---------------------------

30 °C	303	0.00330033	3.7	8.15	2.202703	0.7896851	8.314	-1989.33	-1.98933
40 °C	313	0.00319489	2.3	8.85	3.847826	1.3475083	8.314	-3506.6	-3.5066
50 °C	323	0.00309598	2	9	4.5	1.5040774	8.314	-4039.08	-4.03908

5.0 Fields of applications:

Due to improved surface area, functional groups, mechanical strength, porosity, swelling and biocompatibility of IPN and SIPN system based on any natural and synthetic polymers can be applied to serve sophisticated duties such as sustained release, drug loading/delivery to targeted sites, biomedical use sorption of dyes and heavy metal ion (Lohani et. al., 2014&E.S. Dragan, 2014).Some potential fields of application for IPN and SIPN systems are given in the **table 6**.

Table 6: Some reported applications of IPN and SIPN systems.

S.N.	System	Polymers	application	Reference
1	IPN Hydrogel	Polyacrylate and polyethylene glycol.	Removal of Ni ²⁺ , Cr ³⁺ , and Cd ²⁺ ions	Tang et. al., 2009
2	IPN Hydrogel	Acrylic acid and hydroxyl ethyl methacrylate.	Removal of congo red and methyl violet from water	Mandal and Ray, 2013
3	Semi-IPN Microspheres and film	Chitosan and polyethylene glycol.	Biodegradable drug vehicle	Gunbas et. al., 2012
4	IPN scaffold	Chitosan and polyethylene glycol.	Wound dressing	Sinha et. al., 2012
5	IPN microspheres	Locust bean gum and poly vinyl alcohol.	Controlled release of orally administered drug	Kaity et. al., 2013
6	Semi-IPN microspheres	Sodium alginate and N-isopropyl acrylamide.	Controlled drug release	Reddy et. al., 2008
7	Spongy semi-IPN	Polyethylene glycol and poly 2-hydroxy ethyl methacrylate.	Adsorption of blood protein	A.K. Bajpai, 2007
8	IPN Hydrogel	Gelatine and polylactic	Engineering of bone	A. Fathi et al.,

		ethylene oxide fumarate.	tissue	2013
9	Semi-IPN hydrogel	Polyaspartic acid and polyacrylic acid	Agricultural, biomedical environmental, and Pharmaceutical	Zhao et. al., 2010
10	Semi-IPN microparticles	Polymethacrylic acid and chitosan.	Delivery of insulin orally	Sajeesh and Sharma, 2006

6.0 Conclusion:

In this work, semi-IPN microspheres were successfully prepared by w/o emulsification method containing natural heteropolysaccharide katira gum and synthetic polymer PVA. Which is confirmed by various instrumental methods of characterisation. The semi-IPN shows maximum swelling at 10 pH and swelling is governed by pseudo second order kinetic model. Prepared microspheres were applied for adsorptive removal of BBY cationic azo dye upto 96.92 % from water. The adsorption process followed pseudo second order kinetic model and freundlich isotherm model. Negative value of Gibbs free energy change and positive value of enthalpy change suggested spontaneity and endothermic nature of the process from 30 to 50 °C temperature. Entropy change was found to be positive 103.53 J/mol indicating the increased randomness after adsorption. As discussed in the **table 6** that IPN or SIPN materials having crosslinked natural and synthetic polymers have been prepared by many researchers to render different duties. The fields of application for these materials are vast from medical, pharmaceutical, environmental to agricultural and so on. So, interpenetrating materials can be prepared by taking desired polymers to tune their properties for particular application. Biodegradability, biocompatibility and eco-friendly nature along with ease of preparation and lower cost make them materials of choice for researchers to render different duties.

References

- 1 A Pourjavadi, R. Soleyman, G.R. Barajee, "Novel nanoporous superabsorbent hydrogel based on poly (acrylic acid) grafted onto salep: synthesis and swelling behavior." *Starch-Stärke* 60(9) (2008) 467-475. doi: 10.1002/star.200700706.
- 2 A. Gandini, "Furans as offspring of sugars and polysaccharides and progenitors of a family of remarkable polymers: a review of recent progress." *Polymer Chemistry*, 2010, 1, 245-251. doi:10.1039/b9py00233b
- 3 Ahmed Samer Elfeky, Hanan Farouk Youssef and Ahmed ShafekElzaref, "Adsorption of Dye from Wastewater onto ZnO Nanoparticles-Loaded Zeolite: Kinetic, Thermodynamic and Isotherm Studies." *Z. Phys. Chem.* (2019) 1342. doi.org/10.1515/zpch-2018-1342.

- 4 Ali Fathi, Sherry Lee, Xia Zhong, Nicholas Hon, Peter Valtchev, FaribaDehghani, "Fabrication of interpenetrating polymer network to enhance the biological activity of synthetic hydrogels." *Polymer* 54 (2013) 5534-5542. doi.org/10.1016/j.polymer.2013.08.052.
- 5 Alka Lohani, Garima Singh, Shiv Sankar Bhattacharya, and Anurag Verma, "Interpenetrating Polymer Networks as Innovative Drug Delivery Systems." *Journal of Drug Delivery* Volume 2014, Article ID 583612, 1-11 pages, [doi:10.1155/2014/583612](https://doi.org/10.1155/2014/583612)
- 6 Anil K Bajpai, "Blood protein adsorption onto macroporous semi-interpenetrating polymer networks (IPNs) of poly (ethylene glycol) (PEG) and poly (2-hydroxyethyl methacrylate) (PHEMA) and assessment of in vitro blood compatibility." *Polymer International*, 56:231–244 (2007). DOI: [10.1002/pi.2137](https://doi.org/10.1002/pi.2137).
- 7 Arnab K. Ojha, DebabrataMaiti, Krishnendu Chandra, Subhas Mondal, Debsankar Das Sadhan K. Roy, Kaushik Ghosh, and Syed S. Islam, "Structural assignment of a heteropolysaccharide isolated from the gum of *Cochlospermum religiosum* (Katira gum)." *Carbohydrate Research* 343 (2008) 1222–1231. doi.org/10.1016/j.carres.2008.03.010.
- 8 Arnab K. Ojha, DebabrataMaiti, Krishnendu Chandra, Subhas Mondal, Debsankar Das Sadhan K. Roy, Kaushik Ghosh and Syed S. Islam, "Structural assignment of a heteropolysaccharide isolated from the gum of *Cochlospermum religiosum* (Katira gum)". *Carbohydrate Research* 343 (2008) 1222–1231. [doi: 10.1016/j.carres.2008.03.010](https://doi.org/10.1016/j.carres.2008.03.010)
- 9 Asgher, M., & Bhatti, H. N. (2012). Evaluation of thermodynamics and effect of chemical treatments on sorption potential of citrus waste biomass for removal of anionic dyes from aqueous solutions. *Ecological Engineering*, 38, 79–85.
- 10 Bidyadhar Mandal, Samit Kumar Ray, "Synthesis of interpenetrating network hydrogel from poly (acrylic acid-co-hydroxyethyl methacrylate) and sodium alginate: Modeling and kinetics study for removal of synthetic dyes from water." *Carbohydrate Polymers* 98 (2013) 257–269. doi.org/10.1016/j.carbpol.2013.05.093.
- 11 Crini G, Badot PM. Application of chitosan, a natural amino polysaccharide, for dye removal from aqueous solutions by adsorption processes using batch studies: a review of recent literature. *Prog Polym Sci* 2008; 33:399–447.
- 12 E. W. Hansen and K. H Holm and D. M. Jahr, K. Olafsen and Aa. Stori, "Reaction of poly (vinyl alcohol) and dialdehydes during gel formation probed by ¹H NMR, a kinetic study." *Polymer* Vol. 38 No. 19, pp. 4863 -4871, (1997). PII: S0032-3861 (97)00002-5
- 13 Ecaterina Stela Dragan, "Design and applications of interpenetrating polymer network hydrogels. A review". *Chemical Engineering Journal* 243 (2014) 572–590. doi.org/10.1016/j.cej.2014.01.065

- 14** G.L. Dotto, L.A.A. Pinto, "Adsorption of food dyes onto chitosan: Optimization process and kinetic." *Carbohydrate Polymers* 84 (2011) 231–238.
- 15** Herman S. Mansur, Carolina M. Sadahira, Adriana N. Souza, Alexandra A.P. Mansur, "FTIR spectroscopy characterization of poly (vinyl alcohol) hydrogel with different hydrolysis degrees and chemically crosslinked with glutaraldehyde, *Materials Science and Engineering C* 28 (2008) 539–548. [doi: 10.1016/j.msec.2007.10.088](https://doi.org/10.1016/j.msec.2007.10.088).
- 16** Hu Tu, Yi Yu, Jiajia Chen, Xiaowen Shi, Jialin Zhou, Hongbing Deng, and Yumin Du, "Highly cost-effective and high-strength hydrogels as dye adsorbents from natural polymers: chitosan and cellulose." *Polymer Chemistry*, 2017, 8(19), 2913–2921. [doi:10.1039/c7py00223h](https://doi.org/10.1039/c7py00223h)
- 17** Ismail Dogan Gunbas, UmranAydemirSezer, Sultan Gülcelz, İsmetDelilogluGurhan, and NesrinHasirci, "Semi-IPN Chitosan/PEG Microspheres and Films for Biomedical Applications: Characterization and Sustained Release Optimization." *Industrial & Engineering Chemistry Research*, 2012, 51, 11946–11954. doi.org/10.1021/ie3015523.
- 18** Jana S, Ray J, Mondal B, Pradhan SS, Tripathy T, pH-responsive adsorption/desorption studies of organic dyes from their aqueous solutions by Katira gum-cl-poly (acrylic acid-co-N-vinyl imidazole) hydrogel, *Colloids and Surfaces A: Physicochemical and Engineering Aspects* (2018) 553, 472-486, doi.org/10.1016/j.colsurfa.2018.06.001
- 19** K. Mallikarjuna Reddy, V. Ramesh Babu, K. S. V. Krishna Rao, M. C. S. Subha, K. Chowdoji Rao, M. Sairam, T. M. Aminabhavi, "Temperature Sensitive Semi-IPN Microspheres from Sodium Alginate and N-Isopropylacrylamide for Controlled Release of 5-Fluorouracil." *Journal of Applied Polymer Science*, Vol. 107, 2820–2829 (2008). [DOI: 10.1002/app.27305](https://doi.org/10.1002/app.27305).
- 20** Katime I, Valderruten N, Quintana JR, "Controlled release of aminophylline from poly (N-isopropyl acrylamide-co-itaconic acid) hydrogels." *Polymer International* 2001, 50, 869–874. [doi:10.1002/pi.707](https://doi.org/10.1002/pi.707).
- 21** L. Li, W. Smitthipong and H. Zeng, "Mussel-inspired hydrogels for biomedical and environmental applications." *Polymer Chemistry*, 2014, 6, 353-358. [doi:10.1039/c4py01415d](https://doi.org/10.1039/c4py01415d)
- 22** Luo, X., Zeng, J., Liu, S., Zhang, L., "An effective and recyclable adsorbent for the removal of heavy metal ions from aqueous system: magnetic chitosan/cellulose microspheres." *Bioresource Technology* (2015), 194, 403-406. [dx.doi.org/10.1016/j.biortech.2015.07.044](https://doi.org/10.1016/j.biortech.2015.07.044)
- 23** M. Ghaedi, A. M. Ghaedi, M. Hossainpour, A. Ansari, M. H. Habibi and A. R. Asghari, "Least square-support vector (LS-SVM) method for modeling of methylene blue dye adsorption using copper oxide loaded on activated carbon: kinetic and isotherm study, *J. Ind. Eng. Chem.*, 2014, 20(4), 1641–1649. doi.org/10.1016/j.jiec.2013.08.011.

- 24** M. Sinha, R. M. Banik, C. Haldar, and P. Maiti, "Development of ciprofloxacin hydrochloride loaded poly (ethylene glycol)/chitosan scaffold as wound dressing," *Journal of Porous Materials*, vol. 20, pp. 799–807, 2013. [doi:10.1007/s10934-012-9655-1](https://doi.org/10.1007/s10934-012-9655-1).
- 25** Mamoni Dash, Marcella Ferri, Federica Chiellini, "Synthesis and characterization of semi-interpenetrating polymer network hydrogel based on chitosan and poly(methacryloylglycylglycine)." *Materials Chemistry and Physics* 135 (2012) 1070-1076, doi: [10.1016/j.matchemphys.2012.06.019](https://doi.org/10.1016/j.matchemphys.2012.06.019)
- 26** Pietro Matricardi, Ilenia Onorati, TommasinaCoviello, Franco Alhaique, "Drug delivery matrices based on scleroglucan/alginate/borax gels," *International Journal of Pharmaceutics* 316 (2006) 21–28, doi: [10.1016/j.ijpharm.2006.02.024](https://doi.org/10.1016/j.ijpharm.2006.02.024)
- 27** Qunwei Tang, Xiaoming Sun, Qinghua Li, Jihuai Wu and Jianming Lin, "Synthesis of polyacrylate/polyethylene glycol interpenetrating network hydrogel and its sorption of heavy-metal ions". *science and technology of advanced materials* 10 (2009) 015002.[doi:iopscience.iop.org/1468-6996/10/1/015002](https://doi.org/10.1016/j.ijpharm.2006.02.024).
- 28** Sajeesh S., Chandra P. Sharma, "Interpolymer Complex Microparticles Based on Polymethacrylic Acid-Chitosan for Oral Insulin Delivery." *Journal of Applied Polymer Science*, Vol. 99, 506 –512 (2006) DOI [10.1002/app.22311](https://doi.org/10.1002/app.22311).
- 29** Sanping Zhao, Feng Zhou, Liyan Li, Mengjie Cao, DanyingZuo, Hongtao Liu, "Removal of anionic dyes from aqueous solutions by adsorption of chitosan-based semi-IPN hydrogel composites." *Composites: Part B* 43 (2012) 1570–1578. DOI: [10.1016/j.compositesb.2012.01.015](https://doi.org/10.1016/j.compositesb.2012.01.015).
- 30** Santanu Kaity, Jinu Isaac, Animesh Ghosh, "Interpenetrating polymer network of locust bean gum-poly (vinyl alcohol) for controlled release drug delivery." *Carbohydrate Polymers* 94 (2013) 456–467. doi: [10.1016/j.carbpol.2013.01.070](https://doi.org/10.1016/j.carbpol.2013.01.070).
- 31** Soraya Hassanpour¹ &Massoumeh Bagheri, "Dual-responsive semi-IPN copolymer nanogels based on poly (itaconic acid) and hydroxypropyl cellulose as a carrier for controlled drug release". *Journal of Polymer Research* (May 2017) 24:91. DOI [10.1007/s10965-017-1246-z](https://doi.org/10.1007/s10965-017-1246-z).
- 32** Sourbh Thakur, Omotayo A. Arotiba, "Synthesis, swelling, and adsorption studies of pH-responsive sodium alginate–poly (acrylic acid) superabsorbent hydrogel." *Polymer bulletin* (2018) 75, 4587–4606. doi.org/10.1007/s00289-018-2287-0
- 33** Vaneet Kumar, Vishal Rehani, Balbir Singh Kaith and Saruch, "Synthesis of a biodegradable interpenetrating polymer network of Av-cl-poly(AA-ipn-AAm) for malachite green dye removal: kinetics and thermodynamic studies." *The Royal Society of Chemistry Advances*, 2018, 8, 41920–41937. DOI: [10.1039/c8ra07759b](https://doi.org/10.1039/c8ra07759b).

- 34** Wang, D., Williams, C. G., Yang, F., & Elisseeff, J. H., "Enhancing the tissue biomaterial interface: Tissue-initiated integration of biomaterials." *Advanced Functional Materials*, (2004a) 14, 1152–1159. [doi:10.1002/adfm.200305018](https://doi.org/10.1002/adfm.200305018).
- 35** Wang, T., Turhan, M., & Gunasekaran, S. Selected properties of pH-sensitive, biodegradable chitosan-poly (vinyl alcohol) hydrogel. *Polymer International*, (2004b), 53, 911–918. DOI: [10.1002/pi.1461](https://doi.org/10.1002/pi.1461)
- 36** Xinyu Hu, Liandong Feng, Wei, AmingXie, Shiming Wang, Jianfa Zhang, Wei Dong, "Synthesis and characterization of a novel semi-IPN hydrogel based on Salecan and poly (N, N-dimethylacrylamide-co-2-hydroxyethyl methacrylate)." *Carbohydrate Polymers* 105 (2014) 135–144. doi: [10.1016/j.carbpol.2014.01.051](https://doi.org/10.1016/j.carbpol.2014.01.051).
- 37** Bhatt, P., Singh, S., Kumar Sharma, S. and Rabiou, S. 2021. Development and Characterization of Fast Dissolving Buccal Strip of Frovatriptan Succinate Monoydrate for Buccal Delivery. *International Journal of Pharmaceutical Investigation*. 11, 1 (Mar. 2021), 69-75. DOI:<https://doi.org/10.5530/ijpi.2021.1.13>.
- 38** Y. Yang, S. Wang, Y. Wang, X. Wang, Q. Wang and M. Chen, "Advances in self-assembled chitosan nanomaterials for drug delivery" *Biotechnology Advances*, 2014, 32(7), 1301-1316. doi: [10.1016/j.biotechadv.2014.07](https://doi.org/10.1016/j.biotechadv.2014.07).
- 39** Yilmaz Y, Pekcan O., "In situ fluorescence experiments to study swelling and slow-release kinetics of disc-shaped poly (methyl methacrylate) gels made at various crosslinker densities." *Polymer* 1998; 39:5351–5357. P II: [S0032-3861\(97\)10106-9](https://doi.org/10.1006/poly.1998.3861)